CHINESE OPTICS LETTERS

Vol. 20, No. 1 | January 2022

Harmonic mode-locked fiber laser based on microfiber-assisted nonlinear multimode interference

Renyan Wang (王仁严), Liang Jin (金 亮)*, Jiazhu Wang (王家柱), Shangzhi Xie (谢尚之), Xiaohui Li (李晓晖), Yingtian Xu (徐英添), He Zhang (张 贺), Xin Zhao (赵 鑫), and Xiaohui Ma (马晓辉)

National Key Laboratory of High-power Semiconductor Lasers, Changchun University of Science and Technology, Changchun 130022, China

*Corresponding author: jinliang@cust.edu.cn

Received June 9, 2021 | Accepted August 2, 2021 | Posted Online October 9, 2021

A novel harmonic mode-locked fiber laser based on nonlinear multimode interference (NL-MMI) in a microfiber-assisted ultrafast optical switch is proposed in this Letter. The microfiber-assisted ultrafast optical switch can be obtained by tapering the splicing point of the graded-index multimode fiber (GIMF) and single-mode fiber, which not only helps to shorten the self-imaging period in GIMF to relax the strict requirement of NL-MMI on the length of multimode fiber, but also improves the harmonic order. In the experiment, with the waist diameter of ~15 μm, the repetition rates of the fiber laser can be stably locked at 285 MHz, corresponding to the 16th-order harmonic mode-locking, with the pulse duration of 1.52 ps. Our results provide novel insight into the design of a high-repetition-rate laser and the application of microfibers in the mode-locking device.

Keywords: multimode interference; optical fiber devices; laser mode-locking.
DOI: 10.3788/COL202220.010601

1. Introduction

Ultrafast fiber lasers of high repetition rate are of interest because of their potential application in various fields such as optical communication, frequency measurement, nonlinear optics, high-speed optical sampling, and data storage[1–5]. However, the repetition rate of the normal ultrafast fiber lasers can reach several tens of megahertz (MHz). Passive harmonic mode-locking (HML) is an effective way to the gigahertz (GHz) repetition rate. Compared with active HML fiber lasers[6–9], the advantages of passive HML are the compact all-fiber structure and high signal-to-noise ratio (SNR)[10,11].

The ultrafast optical switch is the core device of the harmonic mode-locked fiber laser, which is divided into artificial and real saturable absorbers. Nonlinear polarization rotation (NPR) and nonlinear optical loop mirror (NOLM) are the most commonly used artificial ultrafast optical switching, which requires a polarization state of an intracavity fiber[12,13]. The saturable absorption mechanism of the real saturable absorber leads to a low damage threshold, and the real saturable absorber also requires the polarization state in the cavity[14–19].

Recently, mode-locking based on nonlinear multimode interference (NL-MMI) has drawn much attention[20]. This nonlinear saturable absorption mechanism is realized by changing the coupling efficiency from the multimode fiber (MMF) to the single-mode fiber (SMF) by controlling the incident optical power. This ultrafast optical switch realized by changing the coupling efficiency not only does this independent of polarization state, but also has a high damage threshold. Mode-locking based on NL-MMI has been successfully applied to traditional mode-locking, dissipative soliton mode-locking, and Q-switching[21–26]. In the previous study of our group, this method is also used to achieve HML by introducing 150 m long SMF in the cavity[27]. However, the long cavity seriously affects the stability of HML, and the precise control of the length of MMF limits the mode-locking based on the NL-MMI[28–30].

In this Letter, a harmonic mode-locked fiber laser based on a tapered single mode fiber–multimode fiber–single mode fiber (SMS) ultrafast optical switch is proposed. By tapering the splicing point between the MMF and SMF, the period of the self-imaging point is reduced, and the dependence of NL-MMI mode locking on the length of MMF is eliminated. In addition, the tapered SMS helps to improve the nonlinear coefficient in the cavity and realize HML without increasing the fiber in the cavity. In the experiments, due to the limitations of the fusion splicer, high-stability HML with a maximum harmonic order of 16, corresponding to a repetition frequency of 285 MHz and a pulse width of 1.52 ps, is achieved with a minimum waist diameter of 15 μm. This optical switch based on the tapered SMS provides a new way to realize highly stable HML.

2. Theoretical Considerations

The tapered SMS ultrafast switch is fabricated by sandwiching a piece of graded-index MMF (GIMF) (0.1 m length, GI 50/125, YOFC) between two standard SMFs (SM28e, YOFC). The tapering is implemented at the splicing point between the GIMF and SMF, as illustrated schematically in Fig. 1. The incident light from SMF excites a number of high-order modes in the GIMF, the interference of which form self-imaging points periodically in the transmission orientation. The period between adjacent self-imaging points L_π is called beat length.

According to Mafi, the length of a GIMF is chosen exactly as the half-beat length L_π or $L = nL_\pi$, where n is an odd integer, and the relative power transmission is at its minimum value for the linear case. As the injected power increases, the relative power transmission increases as well until it reaches its maximum value. Therefore, lower power signals are attenuated, while higher-power ones are transmitted through, resulting in a power-dependent transmission, which means the proposed SMF-GIMF-SMF configuration has the potential to work as a saturable absorber for mode-locking fiber lasers. The beat length L_π can be obtained from the formula $L_\pi = \pi R/\sqrt{2\Delta}$[31], where Δ is the index step, and R is the core radius of the GIMF. By tapering the GIMF, the beat length L_π will be shortened as the GIMF diameter decreases, as shown in Fig. 2(a), when the diameter of the taper reaches 15 μm, the beat length L_π is about 270 μm, which is nearly three times shorter than that of the taper waist with the diameter of 40 μm. Accordingly, the relationship between the number of self-imaging points per unit length and the waist diameter can be expressed by the equation $p = \lambda_0 L/(n_{\mathrm{GIMF}} D^2_{\mathrm{GIMF}})$[32], where L is the length of GIMF, D is the diameter of GIMF, n_{GIMF} is the refractive index of GIMF, and λ_0 is the central wavelength of incident light. Figures 2(b) and 2(c) show the number of self-imaging points per unit length of GIMF with different waist diameters, and the self-imaging points become denser with the decrease of the waist diameter.

The microfiber is tapered from the splicing point using the arc discharge method. To ensure the uniformity and relatively long length of the microfiber waist, we optimized the discharge time and intensity by a fiber fusion splicer (FSM-100 P+, Fujikura). The advantage of using the fiber fusion splicer to taper the fiber is that it can be accurately positioned at the splicing point for tapering, and the waist diameter can be adjusted by controlling the tapering speed. The diameter profile of the tapered fiber is

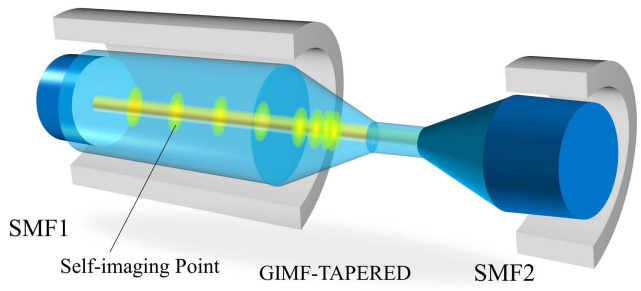

Fig. 1. Schematic diagram of the tapered SMS structure.

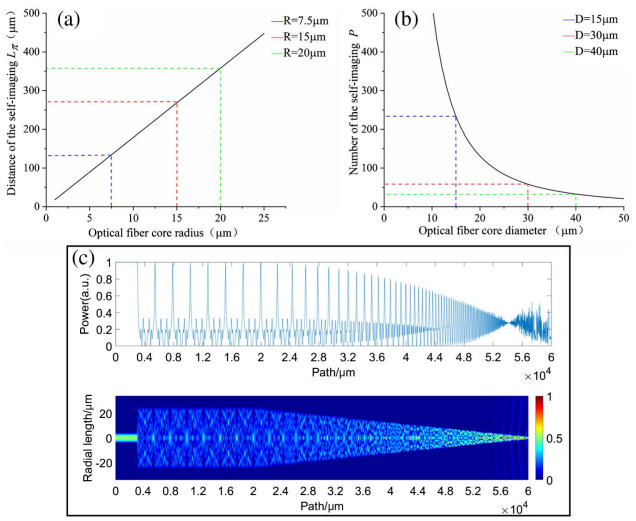

Fig. 2. (a) Relationship between the diameter of GIMF and the beat length. (b) The number of self-imaging points. (c) Self-imaging points in the tapered GIMF.

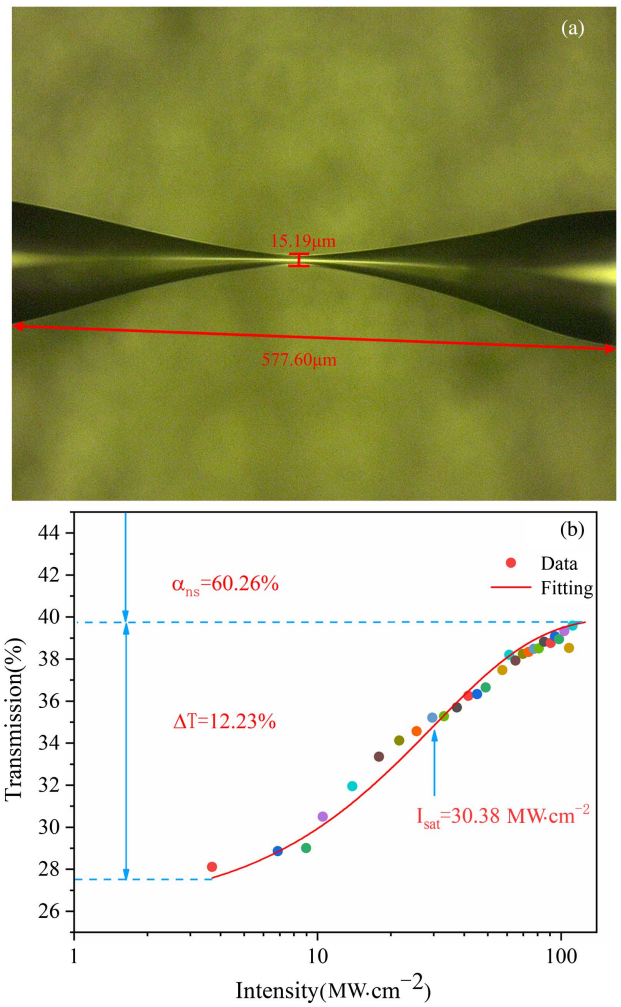

Fig. 3. (a) Microscope image of the tapered SMS. (b) Nonlinear transmission curves of tapered SMS.

shown in Fig. 3(a), and the minimum diameter can reach 15 μm; by adjusting the tapering speed of the fusion splicer, the waist diameter ranges from 15 μm to 40 μm.

To further investigate the nonlinear optical absorption of tapered SMS, an ultrafast fiber laser source is used to excite the NL-MMI. The tapered SMS with a waist diameter of 15 μm is connected with the test source, with the pulse duration of 503 fs and the repetition rate of 15.25 MHz at 1560 nm. The transmittance at ~15 μm increases as the incident power intensity becomes larger due to saturation of absorption, as shown in Fig. 3(b). The saturable absorption curve of the device can be fitted, which is the same as the equation $T = 1 - \Delta T \times \exp(-I/I_{sat}) - \alpha_{ns}$, where T is the transmission, ΔT is the modulation depth, I is the input light intensity, I_{sat} is the saturation intensity, and α_{ns} is the non-saturable loss. The absorption modulation depth is measured as 12.23%, and the value of corresponding saturation fluence is ~30.38 MW·cm^{-2}. The non-saturable loss is 60.26% due to the insertion loss introduced by the taper. The fitting curve agrees well with the experimental data; this shows that the tapered SMS structure has a nonlinear saturable absorption effect.

3. Experiment Section

The ring cavity mode-locked all-fiber laser is schematically presented in Fig. 4. An 80 cm long heavily erbium-doped fiber (Er80-8/125, Liekki) is the gain medium, and the absorption of the gain fiber is 80 dB/m at 1530 nm. The pump source is a single-mode semiconductor laser with the central wavelength of 976 nm (LC96Z600-76, II-IV), which is coupled to the ring cavity by a wavelength-division multiplexer (WDM). A polarization-independent optical isolator (PI-ISO) is used to guarantee the unidirectional propagation of light in the cavity, and a 90/10 fiber coupler couples 10% of the pulse light out of the cavity and generates the laser emission. The output spectrum of the laser is measured using an optical spectrum analyzer (AQ6370D, Yokogawa) and an autocorrelator (FR-103XL, Femtochrome) connected to an 8 GHz digital oscilloscope (DSOV084A, Keysight).

The laser achieves lasing threshold at the pump power of 70 mW. By increasing the pump power gradually to 90 mW and finely tuning the polarization controller (PC), the mode-locked pulse can be obtained. The center wavelength of mode-locking operation is 1558.38 nm, the 3 dB bandwidth is 2.53 nm, and the full width at half-maximum (FWHM) of the pulse is approximately 1.18 ps. The fundamental repetition rate is ~18.21 MHz, and the corresponding pulse interval between two adjacent pulses is 54.06 ns. According to the time bandwidth product (TBP) of the ultrashort pulse, the output pulse is very close to the limitation of the pulse width (the theoretical limit width of the pulse is 1.01 ps). This indicates that the tapered SMS can not only reduce the period of the self-imaging point, making it easy to achieve mode-locking operation, but also compensate for the pulse broadening caused by dispersion chirp in the cavity. To verify that the mode-locking is caused by the tapered SMS ultrafast optical switch, the device is especially removed out of the ring cavity, and no pulse trace can be observed from the oscilloscope. This shows that the tapered SMS contributes to the mode-locking operation.

Continuing to increase the pump power gradually, pulse splitting can be observed by the power clamping effect. HML is obtained by finely adjusting the PC in the cavity. With the pump power increasing to 125 mW, 160 mW, 190 mW, 230 mW, and 300 mW, the harmonic order varies monotonically from fundamental to 2nd, 4th, 6th, 7th, and 16th and corresponds to the repetition rates of 36 MHz, 72 MHz, 104 MHz, 127 MHz, and 285 MHz, respectively. There are four different harmonic orders shown in Fig. 5(a). Figure 5(b) is the pulse width corresponding to each harmonic order. When the pulse splits from the fundamental repetition rate to low-order harmonics, the chirped broadening pulse in the cavity is slightly due to the decrease of the single-pulse energy. However, with the increase of harmonic order, the average power in the cavity also grows, and the pulse broadening caused by the intracavity chirp is serious. Therefore, the harmonic order is proportional to the pulse broadening. Figure 5(c) shows the SNR of the 16th HML when

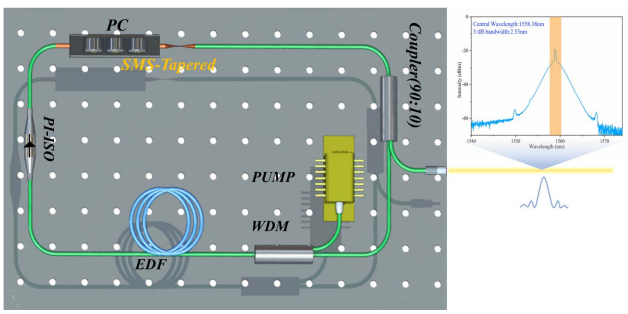

Fig. 4. Diagram of fiber laser based on SMS-tapered ultrafast optical switch.

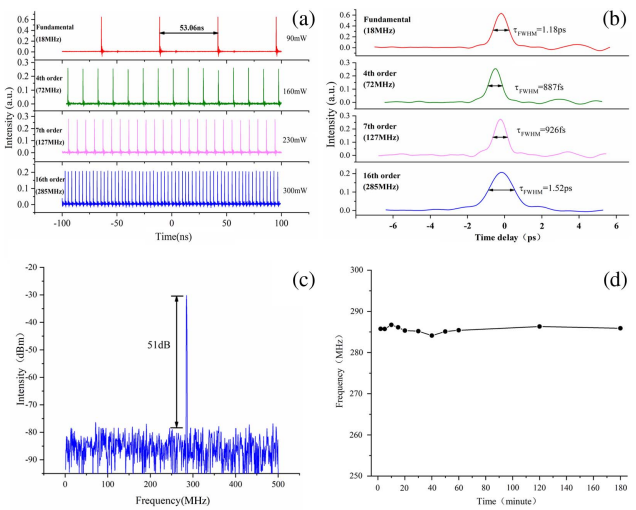

Fig. 5. (a) Pulse trains of various harmonic orders. (b) Pulse profiles of various harmonic orders. (c) RF spectrum of 16th harmonic order. (d) Repetition rates of 16th HML observed at different times.

the waist diameter of the tapered SMS is 15 μm, and the SNR can be stabilized at about 51 dB. Figure 5(d) shows the repetition rates of 16th HML observed at the different times, which verify the stability of the HML.

To investigate the influence of waist diameter on mode-locking, the tapered SMSs with the waist diameters of ~30 μm and ~40 μm are fabricated and introduced in the cavity, with the experiment of HML using tapered SMSs with different waist diameters (other conditions are uniform), and the results are shown in Table 1 and Fig. 6. As can be seen, the pump power is linearly correlated with the harmonic order, and the harmonic order for the waist diameter of 15 μm is higher than that for waist diameters of 30 μm and 40 μm under the same pump power. However, the fundamental repetition rate mode locking can only be realized at the tapered waist diameter of 40 μm. This is mainly because the tapered diameter is inversely proportional

Table 1. Pump Threshold for Harmonic Orders at Different Waist Diameters.

	Pump Threshold (mW)		
Harmonic Order	15 μm	30 μm	40 μm
1	90	110	140
2	125	140	
3		185	
4	160	230	
5		300	
6	195		

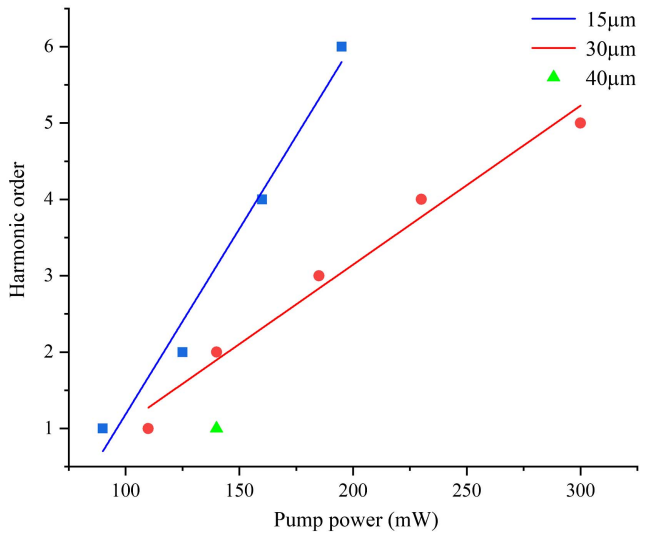

Fig. 6. Relationship between pump power and harmonic order at different waist diameters of tapered SMS.

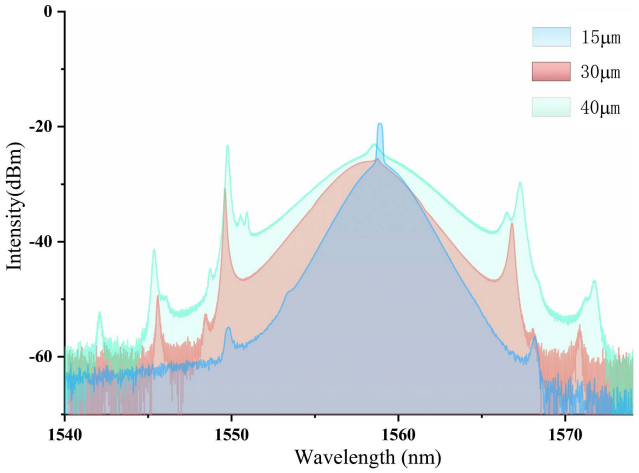

Fig. 7. Spectra of laser with various waist diameters.

to the nonlinear coefficient, and the nonlinear coefficient is proportional to the harmonic order. Therefore, the microfiber promotes the realization of high-order harmonic mode-locking. In this experiment, the waist diameter is limited by arc discharge, and the minimum taper diameter can only reach 15 μm.

Figure 7 shows the mode-locked spectra at different waist diameters of tapered SMS, and all other conditions are identical except for the tapered waist diameter. It can be seen that the tapered waist diameter has little effect on the central wavelength of mode-locking operation. An interesting phenomenon can be found according to the spectra, as the tapered waist diameter decreases, the Kelly sidebands of the spectra gradually disappear. One reason that cannot be ignored is that the tapered fiber in the negative dispersion region can play the role of dispersion compensation. With the decrease of the waist diameter of tapered SMSs, the larger positive dispersion compensation value is provided in the cavity, and the decrease of intracavity dispersion suppresses the generation of Kelly sidebands[33,34]. On the other hand, the CW component exists at the center of the spectrum due to the insufficient modulation depth of the tapered SMS with the waist of 15 μm that was introduced by the insertion loss of tapering[35,36]. It provides a constant phase difference between the solitons to guarantee a stable harmonic mode-locked state[37–39]. The laser cavity can get a high stable harmonic order by further decreasing the diameter of the waist, reducing the insertion loss of tapering, and increasing the pump without the limit of the experimental conditions.

4. Conclusion

In conclusion, a new method of HML based on tapered SMSs is demonstrated in this experiment. Tapering the splicing point between GIMF and SMF not only reduced the period of the self-imaging point, but also relaxed the restriction of mode-locking on the accurate requirement of fiber length. Moreover, the nonlinearity in the cavity is increased, the intracavity dispersion is compensated by tapering of the fibers, and the stable HML is

obtained. In this experiment, the tapered SMS with the waist diameter of 15 μm is introduced as an optical switch to achieve stable HML. The central wavelength of HML fiber laser is 1558.38 nm, with the pulse width of 1.52 ps. The maximum harmonic order can reach 16, and the corresponding repetition rate is 285 MHz. This HML based on tapered SMSs provides a new idea for the application of an all-fiber mode-locking laser in the harmonic regime.

Acknowledgement

This work was supported by the National Natural Science Foundation of China (NSFC) (Nos. 61805023, 61804013, and 61804014).

References

1. U. Keller, "Recent developments in compact ultrafast lasers," Nature **424**, 831 (2003).
2. W. Shi, Q. Fang, X. Zhu, R. A. Norwood, and N. Peyghambarian, "Fiber lasers and their applications," Appl. Opt. **53**, 6554 (2014).
3. C. Kerse, H. Kalaycıoğlu, P. Elahi, Ö. Akçaalan, and F. Ö. Ilday, "3.5 GHz intra-burst repetition rate ultrafast Yb-doped fiber laser," Opt. Commun. **366**, 404 (2016).
4. H. W. Chen, Z. Haider, J. K. Lim, S. Xu, Z. Yang, F. X. KäRtner, and G. Chang, "3 GHz Yb-fiber laser-based, few-cycle ultrafast source at the Ti:sapphire laser wavelength," Opt. Lett. **38**, 4927 (2013).
5. D. Panasenko, P. Polynkin, A. Polynkin, J. V. Moloney, M. Mansuripur, and N. Peyghambarian, "Er-Yb femtosecond ring fiber oscillator with 1.1-W average power and GHz repetition rates," IEEE Photon. Technol. Lett. **18**, 853 (2006).
6. M. S. Kang, N. Y. Joly, and P. ST.J. Russell, "Passive mode-locking of fiber ring laser at the 337th harmonic using gigahertz acoustic core resonances," Opt. Lett. **38**, 561 (2013).
7. G. Sobon, K. Krzempek, P. Kaczmarek, K. M. Abramski, and M. Nikodem, "10 GHz passive harmonic mode-locking in Er-Yb double-clad fiber laser," Opt. Commun. **284**, 4203 (2011).
8. J. Peng, L. Zhan, S. Luo, and Q. Shen, "Passive harmonic mode-locking of dissipative solitons in a normal-dispersion Er-doped fiber laser," J. Lightwave Technol. **31**, 3009 (2013).
9. C. Lecaplain and P. Grelu, "Multi-gigahertz repetition-rate-selectable passive harmonic mode locking of a fiber laser," Opt. Express **21**, 10897 (2013).
10. K. S. Abedin, J. T. Gopinath, L. A. Jiang, M. E. Grein, H. A. Haus, and E. P. Ipeen, "Self-stabilized passive, harmonically mode-locked stretched-pulse erbium fiber ring laser," Opt. Lett. **27**, 1758 (2002).
11. D.-H. Yeh, W. He, M. Pang, X. Jiang, G. Wong, and P. St.J. Russell, "Pulse-repetition-rate tuning of a harmonically mode-locked fiber laser using a tapered photonic crystal fiber," Opt. Lett. **44**, 1580 (2019).
12. Y. D. Ling, Q. Q. Huang, C. H. Zou, Z. J. Yan, and C. B. Mo, "Passively harmonic mode-locked fiber laser with switchable repetition rate based on a 45° tilted fiber grating," Inf. Laser Eng. **47**, 803007 (2018).
13. Y.-Q. Huang, Z.-A. Hu, H. Cui, Z.-C. Luo, A.-P. Luo, and W.-C. Xu, "Coexistence of harmonic soliton molecules and rectangular noise-like pules in a figure-eight fiber laser," Opt. Lett. **41**, 4056 (2016).
14. Q. Huang, T. Wang, C. Zou, M. Alaraimi, A. Rozhin, and C. Mou, "Passively harmonic mode-locked erbium-doped fiber laser at a 580 MHz repetition rate based on carbon nanotubes film," Chin. Opt. Lett. **16**, 020019 (2018).
15. Z. C. Luo, M. Liu, H. Liu, X. W. Zheng, A. P. Luo, C. J. Zhao, H. Zang, S. C. Wen, and W. C. Xu, "2 GHz passively harmonic mode locked fiber laser by a microfiber-band topological insulator saturable absorber," Opt. Lett. **38**, 5212 (2018).
16. J. Koo, J. Park, J. Lee, Y. M. Jhon, and J. H. Lee, "Femtosecond harmonic mode-locking of a fiber laser at 3.27 GHz using a bulk-like, $MoSe_2$-based saturable absorber," Opt. Express **24**, 10575 (2016).
17. A. R. Muhammad, R. Zakaria, M. T. Ahmad, P. Wang, and S. W. Harun, "Pure gold saturable absorber for generating *Q*-switching pulses at 2 μm in thulium-doped fiber laser cavity," Opt. Fiber Technol. **50**, 23 (2019).
18. M. Han, S. Zhang, X. Li, H. Zhang, H. Yang, and T. Yuan, "Polarization dynamic patterns of vector solitons in a graphene mode-locked fiber laser," Opt. Express **23**, 2424 (2015).
19. S. V. Sergeyev, C. Mou, A. Rozhin, and S. K. Turitsyn, "Vector solitons with locked and precessing states of polarization," Opt. Express **20**, 27434 (2012).
20. E. Nazemosadat and A. Mafi, "Nonlinear multimodal interference and saturable absorption using a short graded-index multimode optical fiber," J. Opt. Soc. Am. B **30**, 1357 (2013).
21. E. Nazemosadat and A. Mafi, "Saturable absorption in multicore fiber couplers," J. Opt. Soc. Am. B **30**, 2787 (2013).
22. W. Zhao, G. Chen, W. Li, and G. Wang, "All-fiber saturable absorbers for ultrafast fiber lasers," IEEE Photon. J. **11**, 7104019 (2019).
23. S. Fu, Q. Sheng, X. Zhu, W. Shi, J. Yao, G. Shi, R. A. Norwood, and N. Peyghambarian, "Passive *Q* switching of an all fiber laser induced by the Kerr effect of multimode interference," Opt. Express **23**, 17255 (2015).
24. Z. Wang, D. Wang, F. Yang, and L. Li, "Er doped mode locked fiber laser with a hybrid structure of a step index-graded index multimode fiber as the saturable absorber," J. Lightwave Technol. **35**, 5280 (2017).
25. Y. Fan, D. N. Wang, Z. Wang, L. Li, C. L. Zhao, B. Xu, S. Jin, S. Y. Cao, and Z. J. Fang, "Saturable absorber based on a single mode fiber- graded index fiber-single mode fiber structure with inner microcavity," Opt. Express **26**, 927 (2017).
26. H. Zhang, L. Jin, H. Zhang, Y. Xu, and X. Ma, "All-fiber nonlinear optical switch based on polarization controller coiled SMF-GIMF-SMF for ultra-short pulse generation," Opt. Commun. **452**, 7 (2019).
27. T. Wang, L. Jin, H. Zhang, W. Pan, H. Zhang, Y. Xu, L. Shi, Y. Li, Y. Zou, and X. Ma, "Gigahertz harmonic mode-locked fiber laser based on tunable SMS ultrafast optical switch," Annalen der Physik **532**, 2000018 (2020).
28. H. H. Li, Z. K. Wang, C. Li, J. J. Zhang, and S. Q. Xu, "Mode-locked Tm fiber laser using SMF-SIMF-GIMF-SMF fiber structure as a saturable absorber," Opt. Express **25**, 26546 (2017).
29. Z. Wang, D. N. Wang, Y. Fan, L. Li, C. L. Zhao, B. Xu, S. Jin, S. Y. Cao, and Z. J. Fang, "Stretched graded-index multimode optical fiber as a saturable absorber for erbium-doped fiber laser mode locking," Opt. Lett. **43**, 2078 (2018).
30. Y. Fan, D. N. Wang, Z. Wang, L. Li, C. L. Zhao, B. Xu, S. Jin, S. Y. Cao, and Z. J. Fang, "Saturable absorber based on a single mode fiber-graded index fiber-single mode fiber structure with inner micro-cavity," Opt. Express **26**, 927 (2018).
31. A. Mafi, P. Hofmann, C. J. Salvin, and A. Schülzgen, "Low-loss coupling between two single-mode optical fibers with different mode-field diameters using a graded-index multimode optical fiber," Opt. Lett. **36**, 3596 (2011).
32. F. Tan, J. Liu, R. Sun, and P. Wang, "All-normal-dispersion passively mode-locked Yb-doped fiber laser with multimode interference effect," Chin. J. Lasers **40**, 0402010 (2013).
33. L. Tong, J. Lou, and E. Mazur, "Single-mode guiding properties of subwavelength-diameter silica and silicon wire waveguides," Opt. Express **12**, 1025 (2004).
34. H. H. Liu and K. K. Chow, "Enhanced stability of dispersion-managed mode-locked fiber lasers with near-zero net cavity dispersion by high-contrast saturable absorbers," Opt. Lett. **39**, 150 (2014).
35. J. Wang, Z. Jiang, H. Chen, J. Li, J. Yin, J. Wang, T. He, P. Yan, and S. Ruan, "Magnetron-sputtering deposited WTe_2 for an ultrafast thulium-doped fiber laser," Opt. Lett. **42**, 5010 (2017).
36. J. Wang, Z. Jiang, H. Chen, J. Li, J. Yin, J. Wang, T. He, P. Yan, and S. Ruan, "High energy soliton pulse generation by a magnetron-sputtering-deposition-grown $MoTe_2$ saturable absorber," Photon. Res. **6**, 535 (2018).
37. H. F. Li, S. M. Zhang, J. Du, Y. C. Meng, and X. L. Li, "Passively harmonic mode-locked fiber laser with controllable repetition rate based on a carbon nanotube saturable absorber," Opt. Commun. **285**, 1347 (2012).
38. R. Weill, A. Bekker, V. Smulakovsky, B. Fischer, and O. Gat, "Noise-mediated Casimir-like pulse interaction mechanism in lasers," Optica **3**, 189 (2016).
39. D. Y. Tang, B. Zhao, L. M. Zhao, and H. Y. Tam, "Soliton interaction in a fiber ring laser," Phys. Rev. E **72**, 016616 (2005).